

The effect of boron, copper, and magnesium on the ignition of HEM containing aluminum powder

I V Sorokin¹, A G Korotkikh^{1,2} and E A Selikhova¹

¹ Tomsk Polytechnic University, Tomsk 634050, Russia

² Tomsk State University, Tomsk 634050, Russia

E-mail: korotkikh@tpu.ru

Abstract. The use of metal powder as fuel in high-energy materials (HEM) for propulsion is the most energy-efficient method to increase the burning rate, combustion temperature, and specific impulse. Typically, various dispersity aluminum powders are used in the HEM composition. To improve the ignition and combustion characteristics of the HEM composition it is advisable to use the catalysts (nonmetals, metals or their oxides). This paper presents the experimental data of the HEM samples ignition containing ammonium perchlorate, butadiene rubber, micron powders of aluminum, aluminum-magnesium alloy, as well as nanopowders of amorphous boron, aluminum-copper, and aluminum-boron mixtures. The use of aluminum-copper or aluminum-boron nanopowders in the HEM composition decreases the ignition delay time by 1.3–2.0 times in comparison with Al-based HEM during CO₂ laser initiation. In the case of Al-Mg powder use, the ignition delay time is changed slightly.

1. Introduction

Metal powders (usually micron aluminum) are used as fuels in high-energy materials (HEM) for propulsion due to increasing combustion characteristics of composite solid propellants [1–3] in the combustion chamber of the engine. One of the known regulating ways of the HEM burning rate is the substitution of aluminum micron powder by different metal powders or their oxides, for example, magnesium, titanium, zirconium, cerium, iron, copper, and others [4–7].

Numerous research findings have been published on the ignition and combustion parameters for HEM with different dispersity of metal powder, an oxidizer (most commonly are used NH₄ClO₄, KNO₃), and type of combustible-binder [8–9]. Various heat sources are used to study the processes of ignition and combustion of solid propellants: convective gas blowing, radiant (installations based on various lasers), or conductive heat supply (nichrome wire or spiral) [9, 10].

Promising metal fuels are aluminum powders, which are characterized by different dispersity and passivation method, as well as bimetal powders or mixtures of aluminum and other metals, their alloys, and metal powders with various coatings [11–15]. This paper presents the ignition data of the HEM samples based on ammonium perchlorate (AP), butadiene rubber, containing powders of aluminum, aluminum-magnesium alloy, as well as nanopowders (NP) of amorphous boron, aluminum-copper, and aluminum-boron mixtures.



2. Materials and Methods

2.1. The HEM samples

We studied the HEM samples based on bidispersed AP (fractions with particle size less than 50 μm and 160–315 μm in the ratio of 40/60), inert binder (19.7 wt. %) – butadiene rubber plasticized by transformer oil, and metal powder (15.7 wt. %). The base HEM composition contained micron aluminum powder (ASD-4) with an average particle diameter of 10.8 μm . In the other HEM samples, Al powder was replaced by boron, Al/Mg alloy, or the mechanical mixture of Alex/B and Alex/Cu in the weight ratio of 87/13. Table 1 presents the data of average particle diameter D , the specific surface area S_{sp} and the active metal content for aluminum, copper, and boron NP. The SEM images for metal powders and boron are shown in Figure 1.

Table 1. The mean diameter, specific surface area, and content of active metal of powder.

NP	D , nm	S_{sp} , m^2/g	C_{ac} , wt. %
Alex	90–110	15.5	90.0
B	210–240	8.6	99.5
Cu	50–70	12.0	85.0

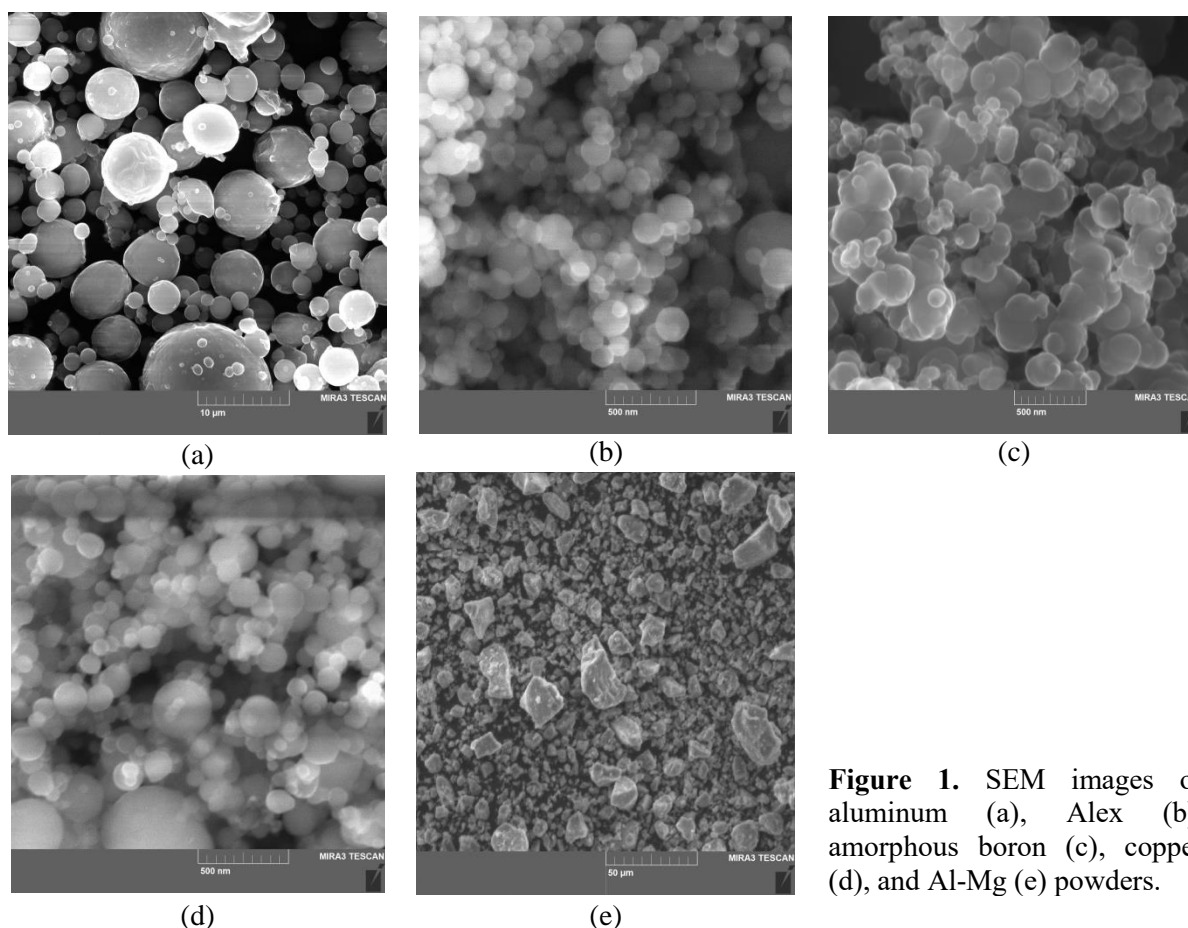


Figure 1. SEM images of aluminum (a), Alex (b), amorphous boron (c), copper (d), and Al-Mg (e) powders.

2.2. Ignition of HEM

The ignition was studied using the setup for the radiant heating based on RLS-200 continuous CO_2 laser with a wavelength of 10.6 μm and thermal power of 200 W (Figure 2). Before testing, the HEM

samples were cut into tablets of 5 mm in height. The flat end surface of the HEM sample was visually monitored for the absence of pores, depressions, and cracks.

The HEM sample (5) was attached to the holder (6). When opening the shutter (3) radiation was focused by the sodium chloride lens (4) to the HEM sample (5). The signals from the photodiodes (7) were transmitted through an analog-to-digital converter (10) (ADC, model E-14-440 manufactured by L-CARD Co.) and recorded using a personal computer (11); afterward, they were processed using the special software (LGraph2, L-CARD Co.). The ignition delay time t_{ign} of HEM was determined by the difference between the signals from two photodiodes (7), one of which registered the appearance of flame near the end surface of the HEM sample and another registered the moment of opening the shutter. The relative error for the ignition delay time values was equal to 5–12 % at the value of confidence probability equal to 0.9.

The average and maximum powers of the laser radiation on the HEM surface were measured using a thermal power sensor (8) (Ophir FL400A-BB-50). To determine a maximum power in the center of the laser beam, we used a diaphragm 2 mm in diameter. The ratio between the maximum and mean thermal power over the area was ~ 1.7 .

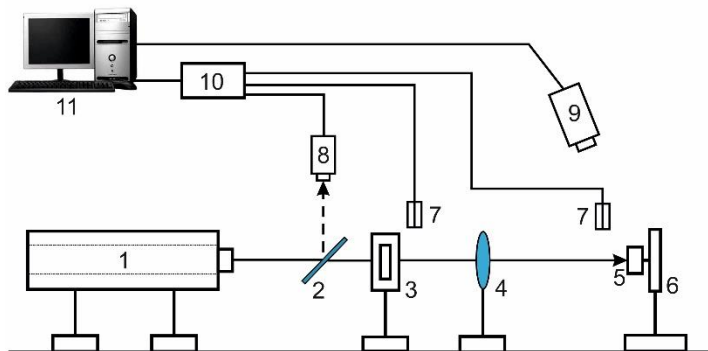


Figure 2. The schematic diagram of experimental setup based on CO₂ laser: 1 – CO₂ laser; 2 – beam-splitting mirror; 3 – shutter; 4 – lens; 5 – HEM sample; 6 – holder; 7 – photodiodes; 8 – thermoelectric sensor of radiation power; 9 – video camera; 10 – ADCs; 11 – PC.

2.3. The effective activation energy of ignition

The effective activation energy during the HEM ignition was determined by solving the inverse heat conduction problem when the sample is heated by a radiative flux following the method of [16]. This method is based on the equation:

$$\ln \left(\frac{t_{ign}}{(1 - T_0 / T_{ign})^2} \right) = \ln \left(\frac{0.35 \cdot Ec}{RQz} \right) + \frac{E}{RT_{ign}}, \quad (1)$$

where t_{ign} is the ignition delay time, s; T_0 is the initial temperature of the HEM sample, K; Q is the specific (per unit weight) heat of the chemical reactions, J/kg; z is the pre-exponential factor, 1/s; E is the effective activation energy, J/mol; c is specific thermal capacity, J/(kg·K); R is the universal gas constant, J/(mole K).

The ignition temperature on the HEM sample surface is determined from the equality condition of the heat release rate in chemical reactions in the reaction volume and the conductive heat flux into the depth of the cold sample. It can be determined by the following formula [16]:

$$T_{ign} = T_0 + 1.2q \sqrt{\frac{t_{ign}}{\lambda \cdot c \cdot \rho}}, \quad (2)$$

where q is the radiative heat flux density, W/cm²; λ , ρ are the thermal conductivity and the density of the HEM sample, W/(m·K), and kg/m³, respectively. The activation energy E and the product of the

thermal effect on the pre-exponent Qz are determined by the slope $\text{tg}\alpha$ of the dependence of

$\ln\left(\frac{t_{ign}}{(1-T_0/T_{ign})^2}\right)$ on $\frac{1}{T_{ign}}$ and its intersection with the ordinate axis at the temperature of T_{ign0} .

3. Results and discussion

3.1. Ignition delay time

The dependences of the ignition delay time of the HEM samples vs. the heat flux density were determined and shown in Figure 3.

The experimental dependences obtained were fitted to a power function of the following form:

$$t_{ign} = A \cdot q^{-B}, \quad (3)$$

where t_{ign} is the ignition delay time of the HEM sample, ms; q is the heat flux density, W/m^2 ; A , B are fitted constants.

Fitted constants and determination coefficient R^2 for the experimental data are given in Table 2.

Table 2. Fitted constants of eq. (3) and determination coefficient.

HEM sample	$A, \cdot 10^5$	B	R^2
ASD-4	0.48	1.39	0.96
Alex/B	1.55	1.73	0.95
Alex/Cu	1.25	1.70	0.98
Al/Mg	0.36	1.35	0.95

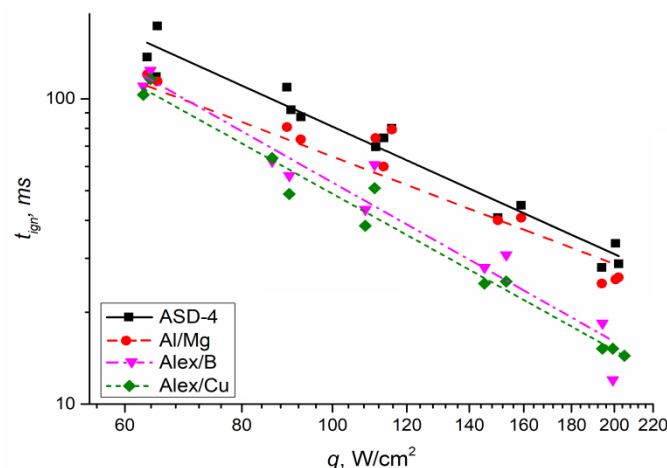


Figure 3. The ignition delay time of the HEM samples vs. the heat flux density.

The experimental results of the study depicted that using metal fuels of Alex/B, Alex/Cu and Al-Mg alloy in the HEM composition reduces the ignition delay time t_{ign} of the HEM samples in the range of heat flux density $q = 60\text{--}200 \text{ W}/\text{cm}^2$ in comparison with the HEM sample containing Al powder. The 2 wt. % additive of copper and boron NP in the Alex-based HEM allows leads to the decrease of the ignition delay time by 1.4–2.0 and 1.3–1.9 times, respectively. The use of Al-Mg alloy in the HEM sample leads to a decrease in the ignition delay time by 10–13 % in the specified range of q .

The use of boron powder reduces the ignition delay time, which may be because boron powder increases the absorbability of the HEM surface. Note, boron particles are difficult to ignite, however,

due to the small size of boron particles (about 220 nm), such particles are heated quickly and their oxidation begins earlier than oxidation of micron-sized particles due to additional heat supply at the thermal decomposition of AP and oxidation of aluminum nanoparticles. The decrease in the ignition delay time during the heating and ignition of the Alex/Cu-based HEM composition can probably be explained by the presence of an oxide layer of CuO on the initial copper particles since the Al/CuO mixture is a thermite mixture, which allows increasing the heat release during ignition and combustion [14, 15].

3.2. Activation energy

The activation energy, pre-exponential factor, and temperature on the reaction layer of the HEM samples during the ignition were determined. Calculation results are shown in Table 3. The HEM sample, containing Alex/Cu, has the highest activation energy (125 kJ/mol), while those of the Al-Mg-based HEM samples have the lowest energy (50.8 kJ/mol). In this case, the temperature T_{ign0} decreases to 19–45 K with the addition of Cu or boron NP compared with the Al-based HEM sample.

Table 3. Calculation data of the formal kinetic parameters for the HEM samples.

HEM sample	E , kJ/mol	Q_z , W/g	T_{ign0} , K
ASD-4	53.8	7.46×10^8	520
Alex/B	108	4.24×10^{15}	475
Alex/Cu	125	1.80×10^{17}	486
Al-Mg	50.8	5.71×10^8	501

We determined the ignition temperature T_{ign} on the HEM sample surface for each sample within the range of heat flux density of 60–200 W/cm². The ignition temperature for samples with ASD-4 varies from 527 to 631 K with a change in heat flux density from 60 to 200 W/cm². The change in ignition temperature for HEM with Alex/B is 503–538 K, for HEM with Alex/Cu is 494–531 K, and for HEM with Al/Mg is 513–619 K.

Conclusions

This study presents the effect of boron, copper, and magnesium additives on the ignition characteristics of the HEM sample based on AP and butadiene rubber.

It was established that the complete replacement of aluminum powder with Alex/B NP in the HEM sample leads to a 1.3–1.9 times decrease in the ignition delay time in the range of heat flux density of 60–200 W/cm². The ignition delay time decreased by 1.4–2.0 times by using Alex/Cu NP in the HEM sample due to a possible catalytic effect. The use of Al-Mg alloy in the HEM sample leads to a decrease in the ignition delay time by 10–13 % in the specified range of q in comparison with the Al-based HEM sample.

Acknowledgements

The reported study was supported by RFBR according to the research project No. 19-33-90015.

References

- [1] Arkhipov V A, Bondarchuk S S, Korotkikh A G, Kuznetsov V T, Gromov A A, Volkov S A, Revyagin L N 2012 *Combust., Expl., Shock Waves* **48** 625–35
- [2] Berner M K, Talawar M B, Zarko V E 2013 *Combust., Expl., Shock Waves* **49** 625–47
- [3] DeLuca L T, Galfetti L, Severini F, Meda L, Marra G, Vorozhtsov A B, Sedoi V S, Babuk VA 2005 *Combust., Expl., Shock Waves* **41** 680–92
- [4] Chintersingh K-L, Schoenitz M, Dreizin E L 2019 *Combust. Flame* **200** 286–95
- [5] Hashim S A, Karmakar Sr, Roy 2019 *Acta Astronautica* **160** 125–37

- [6] Korotkikh A G, Glotov O G, Arkhipov V A, Zarko V E, Kiskin A B 2017 *Combust. Flame* **178** 195–204
- [7] DeLuca L T 2018 *Defence Technology* **14** 357–65
- [8] Ulas A, Kuo K K, Gotzmer C 2001 *Combust. Flame* **127** 1935–57
- [9] Liang D, Liu J, Zhou J, Wang Y, Yang Y 2016 *J. Energ. Mater.* **34** 297–317
- [10] Ahmad S R, Cartwright M 2014 *Laser Ignition of Energetic Materials* (Wiley) p 304
- [11] Abdellahi M, Jabbarzare S, Ghayour H, Khandan A 2018 *J. Therm. Anal. Calorim.* **131** 853–63
- [12] Sergienko A V, Popenko E M, Slyusarsky K V, Larionov K B, Dzidziguri E L, Kondratyeva E S, Gromov A A 2019 *Propell. Explos. Pyrot.* **44** 217–23
- [13] Cheng L, Huang Ch, Yang Y, Li Y, Meng Y, Li Ya, Chen H, Song D, Artiaga R 2020 *Propell. Explos. Pyrot.* **45** 657–64
- [14] Thiruvengadathan R, Bezmelnitsyn A, Apperson S, Staley C, Redner P, Balas W, Nicolich S, Kapoor D, Gangopadhyay K, Gangopadhyay Sh 2011 *Combust. Flame* **158** 964–78
- [15] Dolgoborodov A Yu, Kirilenko V G, Streletsky A N, Kolbanev I V, Shevchenko A A, Yankovsky B D, Ananyev S Yu, Valliano G E 2018 *Combust. Expl.* **11** 117–24
- [16] Vilyunov V N and Zarko V E 1989 *Ignition of Solids* (Elsevier) p 285